Available online at www.sciencedirect.com
ScienceDirect
Bioorganic & Medicinal Chemistry 15 (2007) 4618–4628
Bioorganic & Medicinal Chemistry

Resisting degradation by human elastase: Commonality of design features shared by 'canonical' plant and bacterial macrocyclic protease inhibitor scaffolds

Arnd B. E. Brauer,[a,b,*] Jeffrey D. McBride,[c] Geoff Kelly,[d] Stephen J. Matthews[e] and Robin J. Leatherbarrow[a,*]

[a]*Department of Chemistry, Imperial College London, South Kensington Campus, London SW7 2AZ, UK*
[b]*Institute of Chemistry and Biochemistry, Free University Berlin, Otto Hahn Building, Thielallee 63, 14195 Berlin, Germany*
[c]*Department of Virology, University College London Hospitals, Windeyer Building, 46 Cleveland Street, London W1T 4JF, UK*
[d]*MRC Biomedical NMR Centre, National Institute for Medical Research, The Ridgeway, Mill Hill, London NW7 1AA, UK*
[e]*Department of Biological Sciences, Imperial College London, South Kensington Campus, London SW7 2AZ, UK*

Received 13 June 2006; revised 26 March 2007; accepted 30 March 2007
Available online 3 April 2007

Abstract—A previously unexplained difference in the resistance to enzymatic hydrolysis of 11-mer Bowman–Birk-type inhibitors of human leukocyte elastase that differ in P1 is found to correlate with the strength of a particular intramolecular hydrogen bond within the inhibitor. This transannular hydrogen bond stabilizes the side chain of the conserved P2 Thr in a 'canonical' +60°-rotamer χ^1 conformation and thereby directs it for a close interaction with the enzyme's catalytic His. As the implications of this NMR analysis are neither limited to this macrocyclic scaffold derived from plant proteins nor to a particular serine protease, we present a unified analysis with inhibitory bacterial depsipeptides of 7–12 residues in length that share key design features for which we propose communal functional explanations.

1. Introduction

Most proteins that inhibit serine proteases achieve this by means of an exposed reactive site loop that complexes the enzyme's active site in a substrate-like manner.[2,3] As the backbone geometry of this binding region is conserved in at least 18 non-homologous families of serine protease inhibitor proteins, it is referred to as the 'canonical' conformation and thought to be an outstanding example of convergent evolution.[2,4,5] While serine protease inhibitors based on macrocyclic peptides are rare,[6] they are very useful models for the design of synthetic inhibitors. Therefore, a focus of research has been the design and utilisation of synthetic macrocyclic peptides that are able to maintain the canonical conformation without needing stabilization from a protein scaffold. Such a minimal canonical inhibitor scaffold has evolved from three decades of research and led to the identification of the isolated reactive site loop of Bowman–Birk-type inhibitor proteins (found in dicotyledonous and monocotyledonous seeds)[7–9] as an independent structural β-hairpin motif[10] that can retain both the three-dimensional structure[11] and much of the biological activity of the corresponding region of the complete protein.[7,8,12] This minimal scaffold has proven to be a useful template for the forced evolution of inhibitors by screening synthetic combinatorial peptide libraries against serine proteases including human leukocyte elastase (HLE).[13–15] HLE has been associated with several pathological conditions including pulmonary emphysema, cystic fibrosis, adult respiratory distress syndrome, rheumatoid arthritis and infectious diseases.[16] Furthermore, elevated levels of elastase activity have been reported for several tumour diseases and cancer cell lines, and are thought to play an important role in tumour invasion and metastasis.[17]

Abbreviations: Ahp, 3-amino-6-hydroxy-2-piperidone; BBI, Bowman–Birk inhibitor; cmY, 3′-chloro-*N*-methyl-tyrosine; dhT, dehydroxyThr; HLE, human leukocyte elastase; mY, *N*-methyl-tyrosine; Orn, ornithine; rms, root mean square; xY, δ1, ε2-disubstituted tyrosine[1].

Keywords: P2 threonine; Human elastase; Bowman–Birk serine protease inhibitor; Depsipeptides.

* Corresponding authors. Tel.: +49 30 838 56023; fax: +49 30 838 56413 (A.B.E.B.); tel.: +44 207 594 5752; fax: +44 207 594 1139 (R.J.L.); e-mail addresses: brauer@chemie.fu-berlin.de; R.Leatherbarrow@imperial.ac.uk

0968-0896/$ - see front matter © 2007 Elsevier Ltd. All rights reserved.
doi:10.1016/j.bmc.2007.03.082

Herein we present a detailed ^{1}H NMR analysis to investigate the structural basis of previously noted differences in hydrolysis rates by elastase with inhibitors having different P1 residues. These inhibitors were identified (or used for comparison) during a forced evolution experiment, in which a template-assisted combinatorial peptide library was screened for inhibitors of human leukocyte elastase.[15] Based on the consensus sequence as derived from the library screen, three P1 variants were selected for chemical synthesis (Table 1) because these represent between them the expectedly identified P1 Ala variant, the unexpectedly identified P1 Thr variant and the unexpectedly not identified P1 Val variant. Val is generally considered the preferred P1 residue for HLE in peptide substrates[18–20] and has, therefore, been the most widely utilised residue at this locus for the design of HLE inhibitors.[21]

2. Results and discussion

2.1. P1 substitutions have subtle conformational effects on the inhibitor scaffold

A comparison of the diagnostic regions of the ^{1}H NMR spectra (Fig. 1) of the three studied P1 variants of the plant-derived minimal inhibitor scaffold (Table 1) indicates that the substitutions result in very subtle structural changes only. The most prominent HN chemical shift changes occur at the substituted P1 position, and in the case of the P1 Val variant also at the P5′ Gln9. As a slightly reduced number of NOE restraints could be determined for the P1 Val variant, the corresponding family of NMR-derived structures is not equally well converged as those of the P1 Ala and P1 Thr variants (rms deviation over the P3–P6′ backbone is 0.66 ± 0.22, 0.36 ± 0.12 and 0.37 ± 0.15 for the respective families of structures; cf. Supplementary Material for details of resonance assignments and structure calculations statistics). While this may indicate a marginal difference in the relative rigidity, all three variants adopt the same overall structure and maintain the canonical conformation as shown in Figure 2 and quantified in Table 2. The pairwise rms deviation over the canonical backbone (P3–P2′) demonstrates the conformational similarities between the peptide variants (<0.40 Å), with the corresponding region of complete BBI proteins (⩽0.45 Å; consistent with the similarity of experimental NMR parameters as shown in the Supplementary Material) and with the binding conformations of either canonical serine protease inhibitor proteins or bacterial macrocyclic inhibitors in complex with elastase (<0.75 Å); there are currently no structural reports of BBI proteins in complex with elastase. These values are similar to the deviation range that exists between the structures of canonical proteins (0.19–0.72 Å, Table 2). The retention of the protein-like three-dimensional structure, in particular of the canonical conformation of serine protease inhibitor proteins around the reactive site, explains the potent HLE inhibition of the peptides because it provides a pre-arranged backbone structure that is complementary to the enzyme's active site.

It is characteristic of the canonical conformation to present a hyper-exposed P1 residue for the primary interaction with the protease,[4,22] which may constitute up to 50% of all intermolecular contacts.[23] In the setting of the studied scaffold, the isosteric Thr and Val side chains are found to be accommodated at the P1-position in different manners. The asymmetric side chain of P1 Thr was found to populate preferably the +60° χ^1 rotamer in which the methyl group points away from the P1 carbonyl. Avoidance of such a steric conflict may be the driving force for this conformation. No defined χ^1 conformation was found for the symmetric Val side chain at P1, which instead populates different conformations as is evident from its intermediate $^3J_{H\alpha H\beta}$ coupling constant of 7 Hz. The minimal protease inhibitor scaffold of this study has been demonstrated to be capable of supporting hyper-exposed P1 residues as diverse as Ala, Thr, Val, Lys[11] and Phe[24] with only subtle changes to the three-dimensional structure of the scaffold. However, one effect of the changes to the P1 residue is that the population of the protein-like conformer is attenuated as the size or hydrophobicity of P1 increases. This is evident from an increased population of alternative conformers as exemplified in Figure 1. In the present series, only an alternative conformer of the P1 Val variant was sufficiently populated to allow complete resonance assignment. The backbone of this conformer appears to contain exclusively *trans* peptide bonds and is therefore markedly different from the geometry of the dominant conformer, which has a *cis*-Pro at P3′. This finding is consistent with the observation of conformational heterogeneity arising from Pro *cis*/*trans* isomerisation in all cases of other variants of this inhibitory scaffold in which complete assignment of alternative conformers was achieved.[24,25] For those cases in which the alternative conformers were—unlike in the variants of the present study—sufficiently highly populated to monitor the action of the cognate enzyme on the mixture of conformers directly by NMR, a selective interaction with and subsequent hydrolysis of the protein-like *cis*-P3′-*trans*-P4′ conformer was observed.[24,25]

2.2. The canonical conformation determines the site of hydrolysis

It is generally considered to be an inherent property of the canonical conformation that the backbone geometry of the reactive site region, but neither the reactive site's primary sequence nor the enzyme's specificity, determines the location of the scissile peptide bond, that is, the site of hydrolysis. The P1 Thr variant peptide is particularly suited to test this paradigm for the inhibitory scaffold of this study for two reasons. First, Thr, unlike Ala and Val, is usually not found at the P1-position of HLE substrates or natural inhibitors. However, a P1 Thr was found from a screen of a combinatorial peptidic library for HLE substrates;[26] the engineered P1 Thr mutants of OMTKY3[27] and BPTI[23] are also potent inhibitors of HLE. Second, the enzyme has to distinguish between the two vicinal Thr residues of the peptide sequence. The NMR analysis of the P1 Thr variant peptide hydrolysed by HLE revealed that the cleaved inhibitor populates approximately four different

Table 1. Sequences and biological activities of the P1 Ala, P1 Thr, and P1 Val variants selected for this study from a forced evolution experiment for inhibitors of human leukocyte elastase (HLE) based on a plant-protein-derived scaffold,[15] and of the structurally related natural macrocyclic inhibitors of bacterial origin for which three-dimensional structures are available (Fig. 2)

Schechter and Berger Nomenclature[70]:	P4	P3	P2	P1	P1′	P2′	P3′ ω in *cis*	P4′	P5′	P6′	P7′	P8′	P9′	Frequency of P1 in library screen	Relative rate of hydrolysis by HLE	K_i (HLE) in nM	K_i (PPE) in nM	K_i (other) in nM
Plant-derived BBI-type scaffold																		
P1 Ala	Nle$_1$	C$_2$	T$_3$	A$_4$	S$_5$	I$_6$	P$_7$	P$_8$	Q$_9$	C$_{10}$	Y$_{11}$			91%	1	65	700	
P1 Thr	Nle$_1$	C$_2$	T$_3$	T$_4$	S$_5$	I$_6$	P$_7$	P$_8$	Q$_9$	C$_{10}$	Y$_{11}$			9 %	4	410	1500	
P1 Val	Nle$_1$	C$_2$	T$_3$	V$_4$	S$_5$	I$_6$	P$_7$	P$_8$	Q$_9$	C$_{10}$	Y$_{11}$			0 %	47	130	6700	
SFTI-1 [P1 Val][71]	G$_1$	R$_2$	C$_3$	T$_4$	V$_5$	S$_6$	I$_7$	P$_8$	P$_9$	I$_{10}$	C$_{11}$	F$_{12}$	P$_{13}$	D$_{14}$			71		
SFTI-1[72]	G$_1$	R$_2$	C$_3$	T$_4$	K$_5$	S$_6$	I$_7$	P$_8$	P$_9$	I$_{10}$	C$_{11}$	F$_{12}$	P$_{13}$	D$_{14}$					0.1 (Trypsin)
Bacterial depsipeptide scaffolds																	IC$_{50}$ (PPE) in nM	
Scyptolin A[50]	Butan-1-ol	A$_1$	T$_2$	T$_3$	L$_4$	Ahp$_5$	T$_6$	cmY$_7$	V$_8$								160	
FR901277[73]	Isopropyl carbonyl	Orn$_1$	T$_2$	dhT$_3$	Ahp$_4$	F$_5$	xY$_6$	V$_7$								12	260	
FR901451[74,75]		T$_1$	T$_2$	L$_3$	K$_4$	F$_5$	P$_6$	S$_7$	D$_8$	W$_9$	D$_{10}$	D$_{11}$				10	270	
A90720A[76]	Sulfo glycerate	DL$_1$	T$_2$	R$_3$	Ahp$_4$	L$_6$	mY$_7$	V$_8$										9 (Trypsin)
Marinostatin[77]	F$_1$	A$_2$	T$_3$	M$_4$	R$_5$	Y$_6$	P$_7$	S$_8$	D$_9$	S$_{10}$	D$_{11}$	E$_{12}$						1.5 (Subtilisin BPN) 300 (Chymotrypsin)

In these bacterial inhibitors, the P2 Thr side chain oxygen is part of a lactone, the presence of which classifies them as depsipeptides. Solid lines indicate covalent bonds; dashed lines indicate the hydrogen bond between the P2 Thr side chain and P5′ backbone amide.

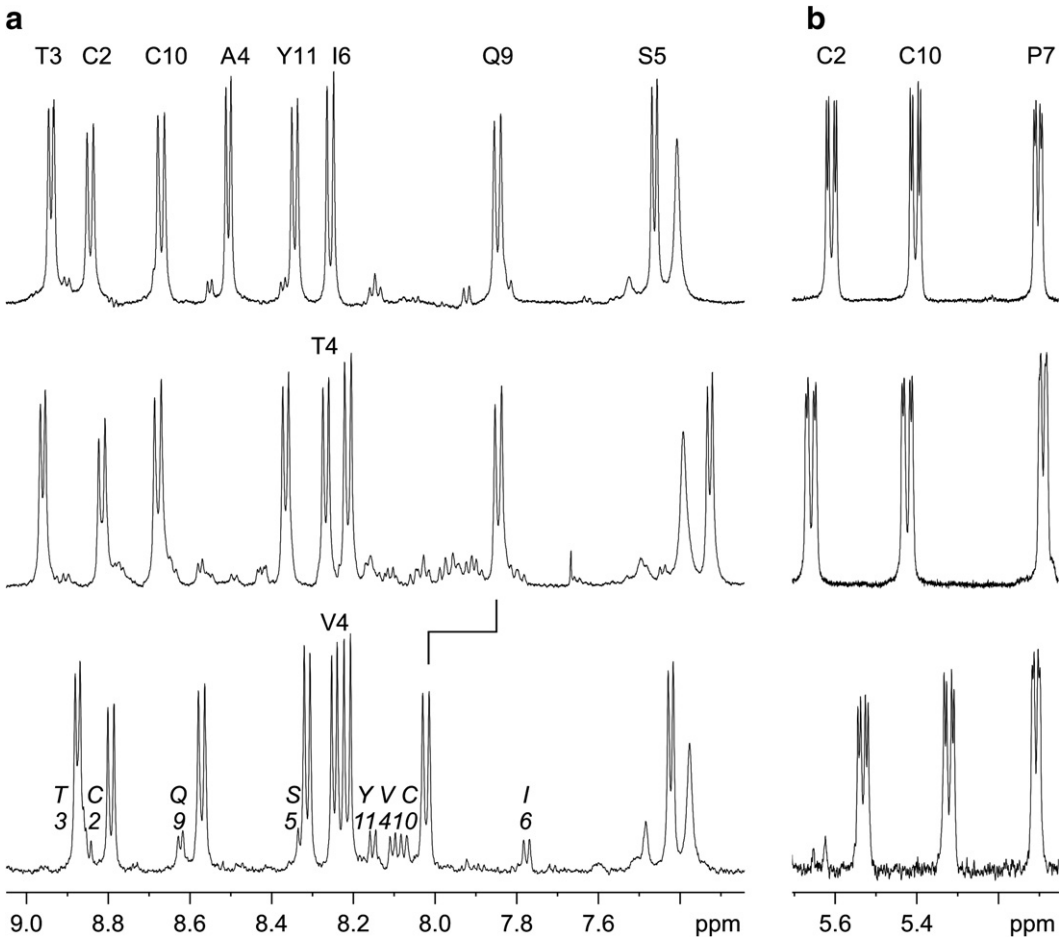

Figure 1. Parts of the ^{1}H NMR spectra of the P1 Ala, P1 Thr and P1 Val variant peptides (from top to bottom) in 90% H_2O/10% D_2O with sequence-labelled backbone HN resonances (a) and in 100% D_2O with labelled downfield shifted Hα resonances (b) at 298 K and pH* 3.8. The displayed non-P1 resonances follow the same order in all the spectra and are labelled only in the top spectrum. A large relative shift of HN P5′ Gln (Q_9) towards the random coil value[82] in the P1 Val variant is indicated by a crossbar. Additional sets of resonances in the spectra indicate the presence of alternative conformations, the small but significant populations of which follow the order P1 Ala < P1 Thr < P1 Val; the resonances of a second conformer of the P1 Val variant are labelled in italics in the bottom spectrum.

conformations, of which only the resonances of the dominant conformer could be fully assigned. No P1′ Ser_5 amide proton resonance could be identified for the assigned dominant conformer, nor were any diagnostic Ser HN/Hβ cross-peaks detected in the spectra (cf. Supplementary Material), even though these should easily be distinguished from the resonances of all other amino acids present due to the characteristic Ser Hβ chemical shifts. This finding indicates that the action of HLE has converted the P1′ Ser_5 amide of the intact inhibitor into a rapidly exchanging additional N-terminus in the cleaved inhibitor. We conclude that the canonical structure of the peptide scaffold successfully enforces the Thr_4–Ser_5 peptide bond as the site of hydrolysis and thus makes Thr_4 the P1 residue as opposed to Thr_3.

2.3. The strength of an intramolecular hydrogen bond of the P2 Thr side chain modulates the stability against enzymatic hydrolysis

The reason that not all expected amino acids at P1 were identified from the screen is that the binding affinity (P1 Ala > P1 Val > P1 Thr) is not correlated with the level of resistance of the intact peptide variants against enzymatic hydrolysis (P1 Ala > P1 Thr >> P1 Val). To analyse this further, details of important potential hydrogen bonds, which have been described in crystal structures of BBI proteins,[28,29] are summarized in Figure 2 and Table 3. Backbone amide proton temperature coefficients and geometric parameters indicate the retention of these protein-like hydrogen bonds in the major protein-like conformer of the peptides in solution. A notable exception is observed for the P1 Val variant's P5′ Gln9 backbone amide proton. From the attenuation of its temperature coefficient, the relative downfield-shift of its proton resonance (highlighted by the crossbar in Fig. 1), fewer observed transannular long-range NOEs and the elongation of its calculated cross-strand hydrogen bond distance with the hydroxyl group of the P2 Thr side chain we conclude that this hydrogen bond is significantly weakened. To test whether this is the structural reason for the increased susceptibility to enzymatic degradation, two experimental NMR-parameters indicative of the variable strength of this hydrogen bond interaction are plotted against the relative rate of enzymatic hydrolysis in Figure 3. For the three anti-HLE variants in Figure 3a, the negative temperature coefficient of the P5′ Gln hydrogen bond donor amide proton

Table 2. Pairwise rms deviations (in Å)[66] between the P1 variants of the protein-derived peptide scaffold of this study, canonical inhibitor protein scaffolds and bacterial scaffold peptides

								Protein-derived peptide scaffold			Protein scaffolds					
											With HLE	With PPE		Bowman–Birk inhibitor		
Inhibitor								P1 Ala variant	P1 Thr variant	P1 Val variant	OMTKY3	Elafin	Ascaris	Lima bean	Mung bean	SFTI-1
In complex with								—	—	—	HLE	PPE	PPE	—	Trypsin	Trypsin
	PDB code							1HD9			1PPF	1FLE	1EAI	1H34		1SFI
		Resolution						NMR	NMR	NMR	1.8 Å	1.9 Å	2.4 Å	2.0 Å	2.5 Å	1.6 Å
Position[70]			P3	P2	P1	P1′	P2′									
Protein-derived peptide scaffold																
P1 Ala variant	1HD9	NMR	C	T	A_4	S	I	—	0.31 ± 0.12	0.39 ± 0.18	0.64 ± 0.10	0.38 ± 0.09	0.41 ± 0.07	0.39 ± 0.09	0.29 ± 0.07	0.40 ± 0.09
P1 Thr variant		NMR	C	T	T_4	S	I	*0.41 ± 0.14*	—	0.39 ± 0.18	0.74 ± 0.07	0.36 ± 0.09	0.35 ± 0.09	0.33 ± 0.11	0.35 ± 0.05	0.45 ± 0.06
P1 Val variant		NMR	C	T	V_4	S	I	*0.60 ± 0.26*	*0.57 ± 0.24*	—	0.67 ± 0.14	0.47 ± 0.16	0.43 ± 0.14	0.40 ± 0.13	0.39 ± 0.11	0.44 ± 0.10
Protein scaffolds																
OMTKY3–HLE[78]	1PPF	1.8 Å	C	T	L_{18}	E	Y				—	0.72	0.65	0.59	0.48	0.37
Elafin–PPE[79]	1FLE	1.9 Å	R	C	A_{24}	M	L					—	0.23	0.30	0.36	0.42
Ascaris–PPE[80]	1EAI	2.4 Å	C	P	L_{31}	M	C						—	0.26	0.31	0.34
Lima bean BBI[81]	1H34	2.0 Å	C	T	K_{26}	S	I	*0.70 ± 0.11*	*0.64 ± 0.10*	*0.74 ± 0.16*				—	0.27	0.25
Mung bean BBI–Trypsin[29]		2.5 Å	C	T	K_{20}	S	I	*0.66 ± 0.10*	*0.69 ± 0.07*	*0.86 ± 0.18*				*0.37*	—	0.19
SFTI-1–Trypsin[72]	1SFI	1.6 Å	C	T	K_{11}	S	I	*0.69 ± 0.10*	*0.72 ± 0.07*	*0.85 ± 0.16*				*0.30*	*0.18*	—
Bacterial depsipeptide scaffolds																
Scyptolin A–PPE[50] (P3–P1)	1OKX	2.8 Å	T	T	L_4	Ahp	T	0.24 ± 0.06*	0.23 ± 0.06*	0.24 ± 0.09*	0.23*	0.30*	0.19*	0.19*	0.16*	0.22*
FR901277–PPE[1] (P3–P1)	1QR3	1.6 Å	Orn	T	dhT_3	Ahp	F	0.22 ± 0.03*	0.23 ± 0.05*	0.26 ± 0.10*	0.19*	0.23*	0.11*	0.15*	0.17*	0.16*
FR901451–PPE[75] (P3–P1)	2CV3	1.9 Å	T	T	L_3	K	F	0.29 ± 0.06*	0.26 ± 0.04*	0.24 ± 0.07*	0.25*	0.34*	0.22*	0.22*	0.21*	0.23*
FR901451–PPE[75] (P3–P2′)								0.64 ± 0.13	0.73 ± 0.08	0.62 ± 0.16	0.23	0.71	0.63	0.59	0.49	0.39

Compared are the backbones of the canonical P3–P2′ segment (plain entries; above the diagonal plus in the last line of the table), and of the complete covalent reactive site loop P3–P6′ segment for BBI-related scaffolds (entries in italic; below the diagonal). Due to the unusual backbone torsion angles imposed by the cyclic P1′ Ahp residue in some of the bacterial scaffolds the superimposition is limited to the P3–P1 segment in these instances (asterisked entries).

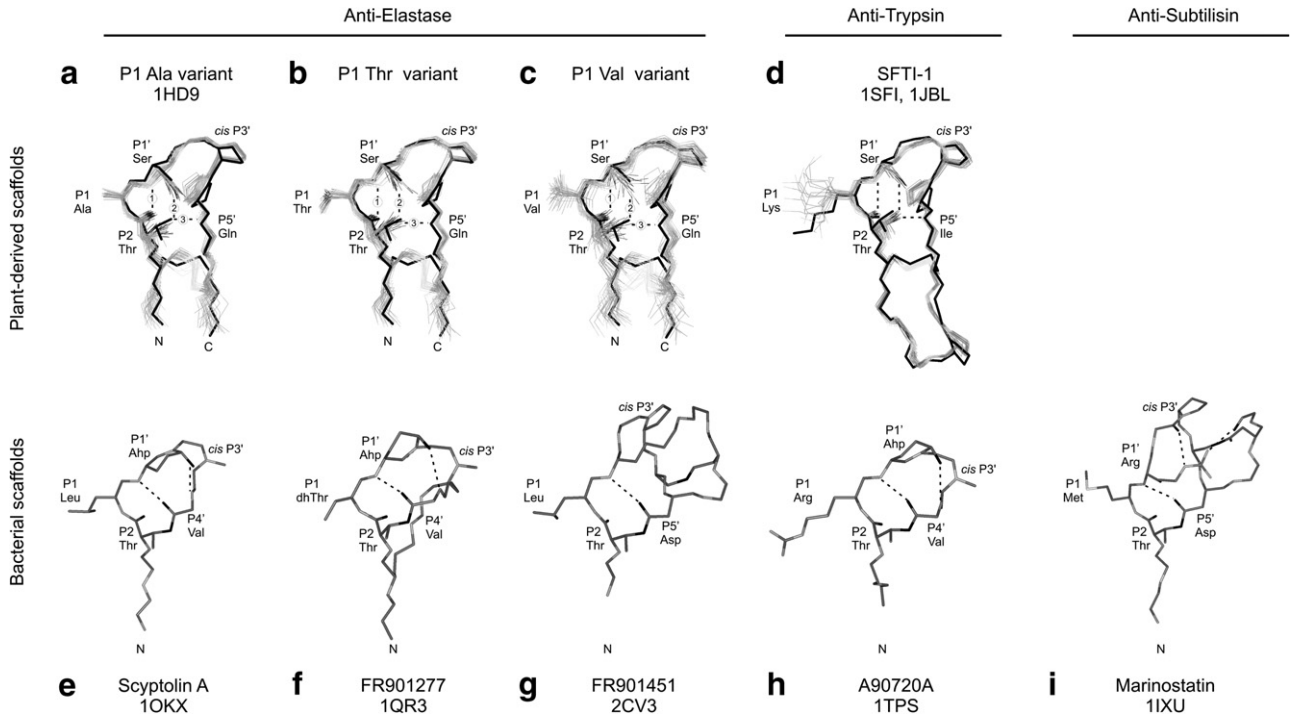

Figure 2. (a–c) Families of NMR-derived solution structures of the P1 variants (lines; O, C, N and S atoms are shown in increasingly lighter shades of grey, respectively) superimposed onto the reactive site loop of Lima bean BBI protein as determined by X-ray crystallography (black sticks; PDB code 1H34; the respective PDB codes for other structures are given in the figure). (d) Family of NMR-derived solution structures of the bicyclic 14-residue sunflower trypsin inhibitor-1 (SFTI-1;[93] lines) superimposed onto its binding structure in complex with bovine trypsin as determined by X-ray crystallography (black sticks[72]). (e, f) Binding structures of the monocyclic 8-residue scyptolin A[50] from the cyanobacterium *Scytonema hofmanni* and the bicyclic 7-residue FR901277[1] from *Streptomyces resistomicificus*, both determined by X-ray crystallography in complex with PPE. (g) Binding structure of the tricyclic 11-residue FR901451 from *Flexibacter* sp. No. 758 as determined by X-ray crystallography in complex with PPE. (h) Binding structure of the monocyclic 8-residue A90720A from the cyanobacterium *Microchaete loktakensis* (X-ray crystal structure in complex with bovine trypsin[52]). (i) NMR solution structure of the bicyclic 12-residue marinostatin active fragment[49] from the marine bacterium *Alteromonas* sp. B-10-31. The orientations of the structures in (a–i), the labelling of the termini and selected residues and the indication of selected potential hydrogen bonds (dashed lines) are chosen to highlight the similar geometry of the binding regions with the hyper-exposed P1 residue and the N-terminal tails, the transannular hydrogen-bond network, the conserved *cis* peptide bond at the N-alkylated P3′ residue, and the conserved P2 Thr side chain that interacts intramolecularly with the P5′ or P4′ residue and adopts in all cases the +60°-rotamer χ^1 conformation. The specific χ^1 values of P2 Thr in the crystal structures are +56° (a–c), +69° (d), +43° (e), +47° (f), +41° (g) and +48° (h).

exhibits a strong correlation with the rate of enzymatic hydrolysis ($r = 0.999$). The chemical shift changes of the same proton confirm this overall trend; the observed slightly increased scatter is to be expected because hydrogen bonding is only one of several parameters that modulate the chemical shift. The evaluation of data for inhibitor variants targeted at trypsin[25,30] and chymotrypsin[24] in Figure 3b and c, respectively, produces similar correlations and suggests that this structure–function relationship is an inherent feature of the inhibitor scaffold of this study, irrespective of the nature of the cognate serine protease. As can be seen in Figure 3c, the geometry-derived identity of the hydrogen bond acceptor as P2 Thr3 $O\gamma_1$ is corroborated because the selective removal of this oxygen atom results in the loss of hydrogen bond no. 3 (numbering as in Table 3). To test whether intramolecular hydrogen bonding in general, or rather hydrogen bond no. 3 in particular, enhances the stability against enzymatic hydrolysis, we also analysed the properties of the only other backbone amide that was identified as a hydrogen bond donor, namely of P1′ Ser5 involved in hydrogen bond no. 1. For the latter, the data show no such correlation (cf. Supplementary Material) and thus substantiate the special role of hydrogen bond no. 3 as a major determinant for the inhibitor's stability. This finding provides quantitative experimental support for a mechanistic hypothesis that we proposed to explain the qualitative observation that anti-chymotryptic variant peptides of the BBI loop with a P2 side-chain $O\gamma_1$ atom (enabling intramolecular hydrogen bond no. 3) are more resistant to enzymatic hydrolysis than P2 variants lacking a side-chain $O\gamma_1$ atom, resulting in Thr as the optimal P2 residue of 26 tested amino acids.[24,31] According to this hypothesis, the strength of hydrogen bond no. 3 directs and stabilizes a close contact between the aliphatic part of the P2 Thr side chain and the imidazole of the enzyme's catalytic His (Fig. 4) and thereby may resist the movement of the catalytic His side chain. Such movement is thought to occur in the course of catalysis, as suggested by theoretical and experimental studies.[32–40] The mobility of the catalytic His side chain has been characterized in several recent studies of series of very high resolution crystal structures of trypsin and elastase complexes that aim to reconstruct the events of the catalytic cycle. For the here concerned early reaction

Table 3. NMR and NMR-derived parameters summarized for a trend analysis of the characteristics of selected potential hydrogen bonds (same numbering as in Fig. 2)

No.	Hydrogen bond	P1	$\Delta\delta/\Delta T$ in ppb/K	$\Delta\delta$ in ppm	Calculated distance in Å		Calculated angle in °		
	D–A				D–A	H–A	D–H–A	H–A–AA	D–A–AA
1	P1′ Ser N–P2 Thr O	Ala	−0.9 ± 0.1	−0.84	2.6	1.8	141	109	96
		Thr	−0.1 ± 0.1	−0.97	3.3	2.5	133	81	77
		Val	−1.3 ± 0.1	−0.87	3.1	2.3	135	87	82
		BBI	−1.1 ± 0.8	−1.00					
		Protein	−1.1 ± 0.8	−1.00					
2	P2 Thr $O\gamma_1$–P1′ Ser $O\gamma$	Ala			2.9	2.7	145	126	123
		Thr			3.0	2.8	140	138	134
		Val			3.3	3.1	115	129	124
3	P5′ Gln N–P2 Thr $O\gamma_1$	Ala	−2.6 ± 0.1	−0.34	4.0	3.1	159	133	134
		Thr	−2.7 ± 0.1	−0.35	4.0	3.1	173	136	135
		Val	−3.9 ± 0.1	−0.17	4.6	3.6	167	141	141
		BBI	−2.6 ± 0.6	−0.69					
		Protein	−1.8 ± 0.1	−0.72					
	Standard criteria for hydrogen bonding[69,84–86]								
	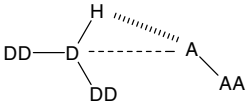		>−4.6		<3.9	<2.5	>90	>90	>90

While the amide proton temperature coefficients ($\Delta\delta/\Delta T$) and deviation from random coil chemical shifts ($\Delta\delta = \delta_{experiment} - \delta_{rc}$)[82] of the P1 Ala and P1 Thr variants closely mirror the corresponding values in both reactive site loops of the complete BBI protein from snail medic seeds (P1 Arg),[83] these parameters as well as the geometric hydrogen bond details (assessed with the program HBPLUS[69] in the average calculated structures reflecting NOE and coupling constant restraints) consistently indicate a relative weakening of hydrogen bond no. 3 in the P1 Val variant. H, D, DD, A and AA are the hydrogen atom, donor atom, donor antecedent, acceptor atom and acceptor antecedent, respectively.

pathway towards acylation, Radisky et al.[41] describe a slight swivelling movement of the His57 side chain in the plane of the ring and conclude that subtle motions of the catalytic Ser and His side chains coordinated with the translation of the substrate reaction centre favour the forward progress of the acylation reaction. Fodor et al.[42] conclude that the shift of the imidazole ring of His57 within its plane is best described with a χ^1 change of approximately 12° for the transition from a Michaelis complex analogue to an acyl-enzyme intermediate. These findings appear consistent with the proposed opposition by the intramolecularly stabilized P2 Thr of complexed intact inhibitors. It is interesting to note that in very high resolution crystallographic studies of deacylation processes, which would occur later in the reaction pathway once the inhibitor's scissile peptide bond had been cleaved, only small or no significant movement of the His57 side chain was observed.[43,44] Consistent with our hypothesis, a recent ab initio study of a self-stabilized model of the chymotrypsin catalytic pocket found that increased conformational rigidity of the substrate resulted in a rise of the activation energy for the formation of the first tetrahedral intermediate, a phenomenon which the authors use to explain the inhibition mechanism of canonical serine protease inhibitors.[45]

While in a recent study Thr was also found to be the optimal anti-tryptic P2 residue in the context of screening SFTI-1 variants,[46] the importance of the resulting intramolecular hydrogen bonds and the interactions with the catalytic machinery is neither a peculiarity of Bowman–Birk-type inhibitors nor limited to serine proteases of the (chymo)trypsin fold. For the subtilisin fold, Radisky et al. found in a combined kinetic and crystallographic study that a P2 Thr → Ala mutation in chymotrypsin inhibitor 2 accelerated the hydrolysis by subtilisin BPN approximately 100-fold and attributed this to the loss of intramolecular hydrogen bonds originating from the P2 side chain.[47]

2.4. Structure–function relationships explain the commonality of design features shared with bacterial macrocyclic inhibitor scaffolds

Another combined kinetic and structural investigation that monitors the effect of the P2 Thr substitution in a structurally related inhibitory depsipeptide, marinostatin,[48,49] is particularly instructive because in this instance the P2 side chain is covalently tethered by lactonization. This arrangement is found in several macrocyclic serine protease inhibitors of bacterial origin that are compared in Table 1 and Figure 2 and include the mono-, bi- and tricyclic elastase inhibitors scyptolin A, FR901277 and FR901451, respectively. Marinostatin, a potent inhibitor of subtilisin BPN, contains two lactones that link the side chains of P2 Thr and P5′ Asp, and of P4′ Ser and P7′ Asp, respectively. The substitution of these lactone links by disulfide bridges barely affects the binding affinity but renders the molecule a temporary inhibitor.[48,49] The authors attribute this to an increased flexibility in particular around the reactive site because of the loss of the strong hydrogen bond donor characteristic of the P1′ backbone amide proton, which is the central atom of the hydrogen bond with the P2 Thr lactone carbonyl.[48] The hydrogen–deuterium exchange rate of this proton was found to be 100-fold

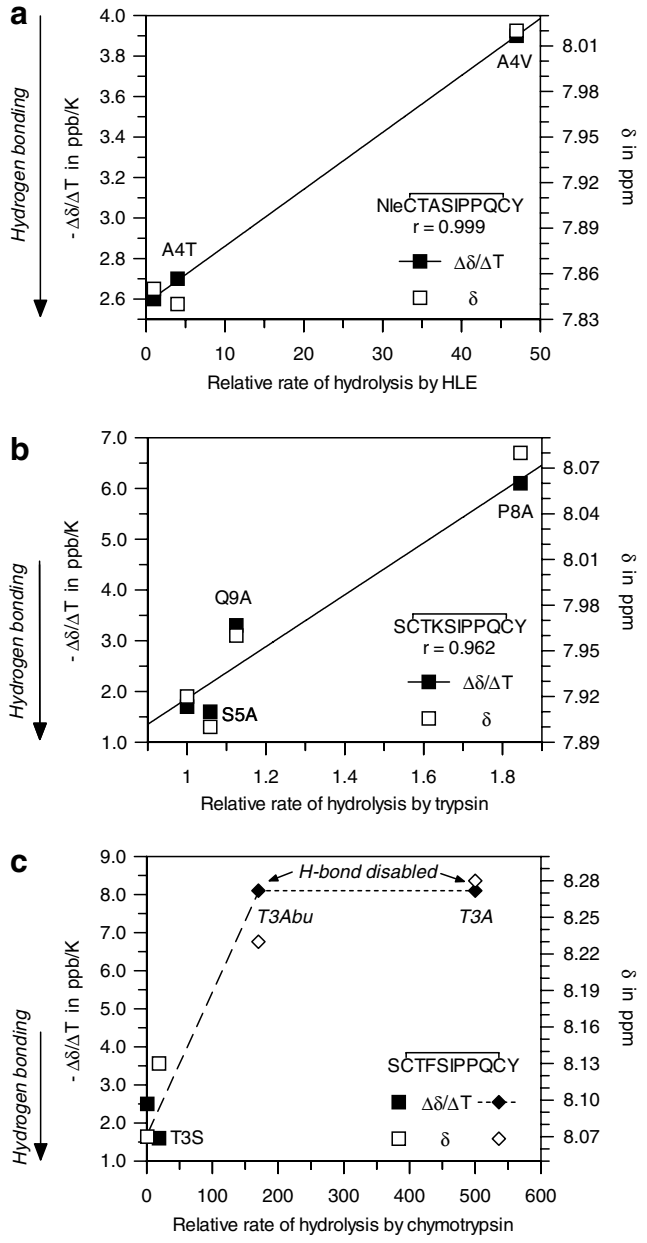

Figure 3. (a) For the P5′ Gln9 backbone amide proton of the three inhibitor variants of this study, two NMR characteristics indicative of the variable strength of the hydrogen bonding interaction (temperature coefficients $\Delta\delta/\Delta T$ and chemical shift δ) are plotted against the relative rate of enzymatic hydrolysis by HLE. A linear correlation coefficient r close to 1 indicates a strong correlation. This trend is verified by the evaluation of data for related inhibitor variants targeted at trypsin[25,30] (b) and chymotrypsin[24] (c). Geometric criteria identify the P2 Thr3 $O\gamma_1$ side chain oxygen atom as the corresponding hydrogen-bond acceptor. The selective elimination of this atom in the *T3Abu* and *T3A* variants (c) has a dual effect: the loss of the hydrogen-bond donor characteristics ($-\Delta\delta/\Delta T \approx 8$ ppb/K; δ within the typical 8.2–8.4 ppm range of average/random coil values[57,82,94]) and acceleration of the enzymatic hydrolysis by up to two orders of magnitude. This finding corroborates the identity of the acceptor and the role of hydrogen bond no. 3 as a major determinant for the inhibitor's stability. The peptide sequences are shown in the diagrams and exchanged amino acids are marked at the individual data points. Arrows at the $-\Delta\delta/\Delta T$ scale indicate the typical hydrogen bond range.[84–86]

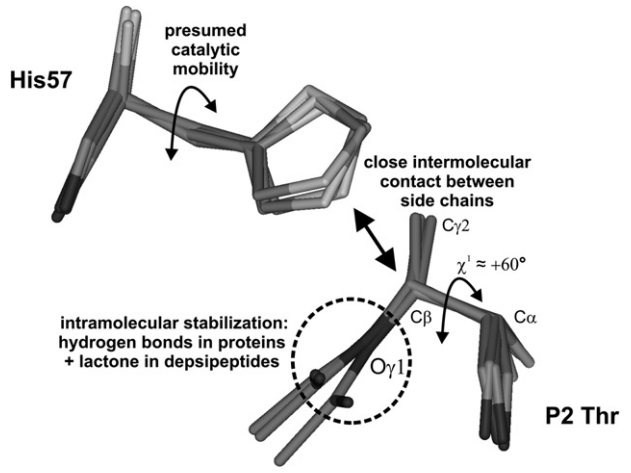

Figure 4. The canonical backbone and side chain conformation of the inhibitors' conserved P2 Thr is demonstrated by the superimposition of four crystal structures in complex with elastase (HLE in complex with the OMTKY3 protein, PDB code 1PPF; PPE in complex with scyptolin A, 1OKX, with FR901277, 1QR3, and with FR901451, 2CV3; O, C and N atoms are shown in increasingly lighter shades of grey, respectively). The hydrophobic part of the P2 Thr side chain is in close contact with the imidazole of the enzyme's catalytic His57; the shortest C–C and C–N distances between these side chains measured in the shown crystal structures range from 3.3 to 3.8 Å, and 3.2 to 3.6 Å, respectively. This contact is directed and stabilized by the intramolecular interactions centered on the P2 Thr side chain oxygen $O\gamma_1$. The strength of this interaction can modulate the rate of enzymatic turnover. This may be rationalized by the presumed movement of the His57 side chain in the course of catalysis.[32–40,43,45,95]

accelerated when this carbonyl functionality is removed by the disulfide substitution.[49] This confirms our conclusion that the degree of intramolecular stabilization at the P2 Thr side chain appears to be a general modulator of the resistance against enzymatic hydrolysis in canonical and quasi-canonical serine protease inhibitors. While this is achieved by hydrogen bonding in plant protein inhibitor scaffolds, some bacterial macrocyclic inhibitors enhance this by an additional intramolecular covalent bond. Despite the evolution of these inhibitors in two different superkingdoms, there is a remarkable commonality of design features as summarized in Table 4 alongside functional explanations proposed based on this unified analysis. A further benefit of the unified analysis is that the unusual features of the bacterial scaffolds (non-DNA encoded amino acids, modifications of the N-terminus, a smaller lactone-cyclized loop) provide inspiration for the design of synthetic scaffolds. An intriguing example is the presence of 3-amino-6-hydroxy-2-piperidone (Ahp) at the P1′-position because—based on crystallographic analyses—this has been proposed to exclude the 'hydrolytic water' and thereby to provide another means of resisting enzymatic hydrolysis[50,51] in addition to rigidifying the binding conformation by its cyclic nature and two transannular hydrogen bonds.[52]

3. Conclusions

While all three anti-HLE P1 variants of a minimal BBI-type inhibitor scaffold were demonstrated to maintain

Table 4. Important design features shared by the plant-derived and bacterial inhibitor scaffolds of comparable size (Fig. 2) and biological potency (Table 1)

Common design feature	Proposed common function
Covalently closed ring of 6–9 amino acid residues which harbours the scissile peptide bond in a (quasi-)canonical setting	(Macro)cyclization greatly enhances the biological potency compared with linear analogues[87,88]
cis peptide bond at the N-alkylated P3′ residue	The *cis* peptide bond reverses the orientation of the peptide backbone to allow for the particular compact covalent scaffold structure; N-alkylation stabilizes the *cis* isomer that preferably interacts with the enzyme;[24,25,48] the balance of *cis*/*trans* isomer populations is dependent on the sequence*,[24,25,30] and nature of cyclization[48,49,89]
P2 Thr side chain adopts a 'canonical' +60°-rotamer χ^1 conformation and interacts via its γ-oxygen atom intramolecularly with the P4′ or P5′ residue	Dual role of P2 Thr side chain for high-affinity binding and high resistance against enzymatic hydrolysis;*,[24,31] the intramolecular interaction of the γ-oxygen atom directs and stabilizes the intermolecular close interaction of the aliphatic part with the side chain of the enzyme's catalytic His
Transannular hydrogen bond network	Rigidifies the bioactive conformation and thereby enhances the resistance against enzymatic turnover*,[24,48,52]
N-terminal tail	Interactions between the residues of the N-terminal tail and the enzyme surface can significantly enhance binding affinity and selectivity;[14,15,90,91] this is also reflected by the variability and modifications of this part of the scaffold in the bacterial inhibitors[1,49,50,52]
Optional additional covalent loop(s)	Conformational guide which appears to facilitate the efficient re-synthesis of the scissile peptide bond by the enzyme[77,92]

By analogy, common functions are proposed for the individual features (*this study).

the canonical binding structure, as was to be expected from their potent inhibition, the previously unexplained difference in the resistance against enzymatic hydrolysis was found to correlate closely with the strength of the transannular hydrogen bond that connects the P2 Thr side chain in the +60° χ^1 rotamer with the P5′ residue. The conclusion that such interactions are general modulators of the resistance against enzymatic hydrolysis was corroborated by reviewing experimental data for a wide range of serine proteases and their cognate P2 Thr-bearing inhibitors. Similar, though covalent, interactions in bacterial depsipeptides provide a strikingly analogous route for stabilization. We believe that further exploitation of this phenomenon and the understanding of the communal construction features could fruitfully impact on the design of synthetic inhibitors.

4. Experimental

The peptides of this study were generated by established solid-phase peptide synthesis methods as described previously.[15] Hydrolysed P1 Thr variant peptide was produced by exposing the intact peptide to a catalytic amount of HLE followed by incubation in aqueous solution at pH 7 and 277 K. Elastase from human polymorphonuclear leukocytes (HLE), a product of Elastin Products Co. Inc., Owensville, MO, USA, was kindly supplied by Dr. Robin Smith, GlaxoSmithKline.

The ^{1}H NMR analysis was performed in aqueous solution (90% H_2O/10% D_2O and 100% D_2O, with 3-(trimethylsilyl)-1-propane sulfonic acid as internal reference) at pH* 3.8 and 298 K. DQF-COSY,[53] TOCSY[54] (mixing time 80 ms), NOESY[55] (mixing time 300 ms) and ROESY[56] (mixing time 300 ms) experiments were performed on a Bruker AMX 600 spectrometer and processed and analysed with X-WinNMR and Aurelia software packages on Silicon Graphics workstations. Following sequential assignment,[57] amide proton temperature coefficients,[58] diastereotopic proton assignment and χ^1 conformations,[59] $^3J_{HNH\alpha}$ coupling constants,[60] and $^3J_{H\alpha H\beta}$ coupling constants[61,62] were analysed as described in the references.[10] All coupling constants were derived from one-dimensional spectra.

Peptide structures were calculated with the program X-PLOR (version 3.851)[63] using a modified version[10] of a standard simulated annealing protocol.[64] The most important modification was the addition of direct refinement against $^3J_{HNH\alpha}$ coupling constants[65] for values >8 Hz during the final conjugate gradient minimisation. No hydrogen bond restraints were used during the calculations. The programs INSIGHT II and WebLab (both Molecular Simulations Inc.), MOLMOL,[66] Swiss-PDBViewer,[67] PROCHECK[68] and HBPLUS[69] were used for the visualisation and analysis of the structures.

Acknowledgments

The authors wish to thank H. Toms and P. Haycock of the University of London 600 MHz NMR facility at Queen Mary College for their expert advice and assistance, R. Cooke for helpful discussions, W. Bode for sending the co-ordinates of mung bean BBI in complex with trypsin, T. Kinoshita and T. Tada for making the co-ordinates 2CV3 available prior to the PDB release and G. Radau for sending information on cyanopeptides. We gratefully acknowledge the financial support of GlaxoSmithKline and the BBSRC.

Supplementary data

Three tables and figures each provide the resonance assignments, structure calculations statistics, comparisons of the secondary chemical shifts and amide proton temperature coefficients of the BBI loop in a protein and the studied peptides, an NMR analysis of the P1 Thr variant hydrolysed by HLE showing a TOCSY spectrum and the control plots corresponding to Figure 3. Supplementary data associated with this article can be found, in the online version, at doi:10.1016/j.bmc.2007.03.082.

References and notes

1. Nakanishi, I.; Kinoshita, T.; Sato, A.; Tada, T. *Biopolymers* **2000**, *53*, 434.
2. Bode, W.; Huber, R. *Eur. J. Biochem.* **1992**, *204*, 433.
3. Bode, W.; Huber, R. *Biochim. Biophys. Acta* **2000**, *1477*, 241.
4. Laskowski, M.; Qasim, M. A. *Biochim. Biophys. Acta* **2000**, *1477*, 324.
5. Rawlings, N. D.; Tolle, D. P.; Barrett, A. J. *Biochem. J.* **2004**, *378*, 705.
6. Maryanoff, B. E. *J. Med. Chem.* **2004**, *47*, 769.
7. McBride, J. D.; Leatherbarrow, R. J. *Curr. Med. Chem.* **2001**, *8*, 909.
8. Qi, R. F.; Song, Z. W.; Chi, C. W. *Acta Biochim. Biophys. Sin.* **2005**, *37*, 283–292.
9. Prakash, B.; Selvaraj, S.; Murthy, M. R.; Sreerama, Y. N.; Rao, D. R.; Gowda, L. R. *J. Mol. Evol.* **1996**, *42*, 560.
10. Brauer, A. B. E.; Kelly, G.; McBride, J. D.; Cooke, R. M.; Matthews, S. J.; Leatherbarrow, R. J. *J. Mol. Biol.* **2001**, *306*, 799.
11. Brauer, A. B. E.; Kelly, G.; Matthews, S. J.; Leatherbarrow, R. J. *J. Biomol. Struct. Dyn.* **2002**, *20*, 59.
12. McBride, J. D.; Watson, E. M.; Brauer, A. B. E.; Jaulent, A. M.; Leatherbarrow, R. J. *Biopolymers* **2002**, *66*, 79.
13. McBride, J. D.; Freeman, N.; Domingo, G. J.; Leatherbarrow, R. J. *J. Mol. Biol.* **1996**, *259*, 819.
14. McBride, J. D.; Freeman, H. N. M.; Leatherbarrow, R. J. *J. Pept. Sci.* **2000**, *6*, 446.
15. McBride, J. D.; Freeman, H. N. M.; Leatherbarrow, R. J. *Eur. J. Biochem.* **1999**, *266*, 403.
16. Bieth, J. G. In *Handbook of Proteolytic Enzymes*; Barrett, A. J., Rawlings, N. D., Woessner, J. F., Eds.; Academic Press: San Diego, 1998, Chapter 15.
17. Achilles, K.; Bednarski, P. J. *Biol. Chem.* **2003**, *384*, 817.
18. Harper, J. W.; Cook, R. R.; Roberts, C. J.; McLaughlin, B. J.; Powers, J. C. *Biochemistry* **1984**, *23*, 2995.
19. Stein, R. L.; Trainer, D. A.; Wildonger, R. A. *Annu. Rep. Med. Chem.* **1985**, *20*, 237.
20. McRae, B.; Nakajima, K.; Travis, J.; Powers, J. C. *Biochemistry* **1980**, *19*, 3973.
21. Edwards, P. D.; Bernstein, P. R. *Med. Res. Rev.* **1994**, *14*, 127.
22. Apostoluk, W.; Otlewski, J. *Proteins Str. Func. Gen.* **1998**, *32*, 459.
23. Krowarsch, D.; Dadlez, M.; Buczek, O.; Krokoszynska, I.; Smalas, A. O.; Otlewski, J. *J. Mol. Biol.* **1999**, *289*, 175.
24. Brauer, A. B. E.; Nievo, M.; McBride, J. D.; Leatherbarrow, R. J. *J. Biomol. Struct. Dyn.* **2003**, *20*, 645.
25. Brauer, A. B. E.; Domingo, G. J.; Cooke, R. M.; Matthews, S. J.; Leatherbarrow, R. J. *Biochemistry* **2002**, *41*, 10608.
26. Harris, J. L.; Backes, B. J.; Leonetti, F.; Mahrus, S.; Ellman, J. A.; Craik, C. S. *Proc. Natl. Acad. Sci. U.S.A.* **2000**, *97*, 7754–7759.
27. Lu, W. Y.; Apostol, I.; Qasim, M. A.; Warne, N.; Wynn, R.; Zhang, W. L.; Anderson, S.; Chiang, Y. W.; Ogin, E.; Rothberg, I.; Ryan, K.; Laskowski, M. *J. Mol. Biol.* **1997**, *266*, 441.
28. Voss, R. H.; Ermler, U.; Essen, L. O.; Wenzl, G.; Kim, Y. M.; Flecker, P. *Eur. J. Biochem.* **1996**, *242*, 122.
29. Lin, G. D.; Bode, W.; Huber, R.; Chi, C. W.; Engh, R. A. *Eur. J. Biochem.* **1993**, *212*, 549.
30. Brauer, A. B. E.; Leatherbarrow, R. J. *Biochem. Biophys. Res. Commun.* **2003**, *308*, 300.
31. McBride, J. D.; Brauer, A. B. E.; Nievo, M.; Leatherbarrow, R. J. *J. Mol. Biol.* **1998**, *282*, 447.
32. Gronenstein, D. G.; Taira, K. *Biophys. J.* **1984**, *46*, 749.
33. Bachovchin, W. W. *Biochemistry* **1986**, *25*, 7751.
34. Ash, E. L.; Sudmeier, J. L.; Day, R. M.; Vincent, M.; Torchilin, E. V.; Haddad, K. C.; Bradshaw, E. M.; Sanford, D. G.; Bachovchin, W. W. *Proc. Natl. Acad. Sci. U.S.A.* **2000**, *97*, 10371.
35. Katona, G.; Wilmouth, R. C.; Wright, P. A.; Berglund, G. I.; Hajdu, J.; Neutze, R.; Schofield, C. J. *J. Biol. Chem.* **2002**, *277*, 21962.
36. Topf, M.; Varnai, P.; Schofield, C. J.; Richards, W. G. *Proteins Str. Funct. Gen.* **2002**, *47*, 357.
37. Kostetskii, P. V. *Biofizika* **2004**, *49*, 595.
38. Topf, M.; Varnai, P.; Richards, W. G. *J. Am. Chem. Soc.* **2002**, *124*, 14780.
39. Topf, M.; Richards, W. G. *J. Am. Chem. Soc.* **2004**, *126*, 14631.
40. Sumi, H.; Ulstrup, J. *Biochim. Biophys. Acta* **1988**, *955*, 26.
41. Radisky, E. S.; Lee, J. M.; Lu, C. J.; Koshland, D. E., Jr. *Proc. Natl. Acad. Sci. U.S.A.* **2006**, *103*, 6835.
42. Fodor, K.; Harmat, V.; Neutze, R.; Szilagyi, L.; Graf, L.; Katona, G. *Biochemistry* **2006**, *45*, 2114.
43. Wilmouth, R. C.; Edman, K.; Neutze, R.; Wright, P. A.; Clifton, I. J.; Schneider, T. R.; Schofield, C. J.; Hajdu, J. *Nat. Struct. Biol.* **2001**, *8*, 689.
44. Liu, B.; Schofield, C. J.; Wilmouth, R. C. *J. Biol. Chem.* **2006**, *281*, 24024.
45. Hudaky, P.; Perczel, A. *Proteins* **2006**, *62*, 749.
46. Hilpert, K.; Hansen, G.; Wessner, H.; Volkmer-Engert, R.; Höhne, W. *J. Biochem. (Tokyo)* **2005**, *138*, 383.
47. Radisky, E. S.; Lu, C. J.; Kwan, G.; Koshland, D. E., Jr. *Biochemistry* **2005**, *44*, 6823.
48. Taniguchi, M.; Kamei, K.; Kanaori, K.; Koyama, T.; Yasui, T.; Takano, R.; Harada, S.; Tajima, K.; Imada, C.; Hara, S. *J. Pept. Res.* **2005**, *66*, 49.
49. Kanaori, K.; Kamei, K.; Taniguchi, M.; Koyama, T.; Yasui, T.; Takano, R.; Imada, C.; Tajima, K.; Hara, S. *Biochemistry* **2005**, *44*, 2462.
50. Matern, U.; Schleberger, C.; Jelakovic, S.; Weckesser, J.; Schulz, G. E. *Chem. Biol.* **2003**, *10*, 997.
51. McDonough, M. A.; Schofield, C. J. *Chem. Biol.* **2003**, *10*, 898.
52. Lee, A. Y.; Smitka, T. A.; Bonjouklian, R.; Clardy, J. *Chem. Biol.* **1994**, *1*, 113.
53. Derome, A. E.; Williamson, M. P. *J. Magn. Reson.* **1990**, *88*, 177.
54. Bax, A.; Davis, D. G. *J. Magn. Reson.* **1985**, *65*, 355.
55. Jeener, J.; Meier, B. H.; Bachman, P.; Ernst, R. R. *J. Chem. Phys.* **1979**, *71*, 4546.
56. Griesinger, C.; Ernst, R. R. *J. Magn. Reson.* **1987**, *75*, 261.
57. Wüthrich, K. *NMR of Proteins and Nucleic Acids*; John Wiley & Sons: New York, 1986.
58. Andersen, N. H.; Neidigh, J. W.; Harris, S. M.; Lee, G. M.; Liu, Z. H.; Tong, H. *J. Am. Chem. Soc.* **1997**, *119*, 8547.

59. Wagner, G.; Braun, W.; Havel, T. F.; Schaumann, T.; Go, N.; Wüthrich, K. *J. Mol. Biol.* **1987**, *196*, 611.
60. Pardi, A.; Billeter, M.; Wüthrich, K. *J. Mol. Biol.* **1984**, *180*, 741.
61. DeMarco, A.; Llinás, M.; Wüthrich, K. *Biopolymers* **1978**, *17*, 617.
62. Cai, M. G.; Huang, Y.; Liu, J. H.; Krishnamoorthi, R. *J. Biomol. NMR* **1995**, *6*, 123.
63. Brünger, A. T. *X-PLOR Version 3.1: A System for X-ray Crystallography and NMR*; Yale University Press: New Haven, 1993.
64. Hofmann, M.; Gondol, D.; Bovermann, G.; Nilges, M. *Eur. J. Biochem.* **1989**, *186*, 95.
65. Garrett, D. S.; Kuszewski, J.; Hancock, T. J.; Lodi, P. J.; Vuister, G. W.; Gronenborn, A. M.; Clore, G. M. *J. Magn. Reson. B* **1994**, *104*, 99.
66. Koradi, R.; Billeter, M.; Wüthrich, K. *J. Mol. Graph.* **1996**, *14*, 51.
67. Guex, N.; Peitsch, M. C. *Electrophoresis* **1997**, *18*, 2714.
68. Laskowski, R. A.; Macarthur, M. W.; Moss, D. S.; Thornton, J. M. *J. Appl. Crystallogr.* **1993**, *26*, 283.
69. McDonald, I. K.; Thornton, J. M. *J. Mol. Biol.* **1994**, *238*, 777.
70. Schechter, I.; Berger, A. *Biochem. Biophys. Res. Commun.* **1967**, *27*, 157.
71. Zablotna, E.; Kret, A.; Jaskiewicz, A.; Olma, A.; Leplawy, M. T.; Rolka, K. *Biochem. Biophys. Res. Commun.* **2006**, *340*, 823.
72. Luckett, S.; Garcia, R. S.; Barker, J. J.; Konarev, A. V.; Shewry, P. R.; Clarke, A. R.; Brady, R. L. *J. Mol. Biol.* **1999**, *290*, 525.
73. Fujie, K.; Shinguh, Y.; Hatanaka, H.; Shigematsu, N.; Murai, H.; Fujita, T.; Yamashita, M.; Okamoto, M.; Okuhara, M. *J. Antibiot. (Tokyo)* **1993**, *46*, 908.
74. Fujita, T.; Hatanaka, H.; Hayashi, K.; Shigematsu, N.; Takase, S.; Okamoto, M.; Okuhara, M.; Shimatani, K.; Satoh, A. *J. Antibiot. (Tokyo)* **1994**, *47*, 1359.
75. Kinoshita, T.; Kitatani, T.; Warizaya, M.; Tada, T. *Acta Crystallogr. F – Struct. Biol. Crystallization Commun.* **2005**, *61*, 808.
76. Burger, M. T.; Bartlett, P. A. *J. Am. Chem. Soc.* **1997**, *119*, 12697.
77. Takano, R.; Imada, C.; Kamei, K.; Hara, S. *J. Biochem. (Tokyo)* **1991**, *110*, 856.
78. Bode, W.; Wei, A. Z.; Huber, R.; Meyer, E.; Travis, J.; Neumann, S. *EMBO J.* **1986**, *5*, 2453.
79. Tsunemi, M.; Matsuura, Y.; Sakakibara, S.; Katsube, Y. *Biochemistry* **1996**, *35*, 11570.
80. Huang, K.; Strynadka, N. C. J.; Bernard, V. D.; Peanasky, R. J.; James, M. N. G. *Structure* **1994**, *2*, 679.
81. Debreczeni, J. E.; Bunkoczi, G.; Girmann, B.; Sheldrick, G. M. *Acta Crystallogr. D* **2003**, *59*, 393.
82. Wishart, D. S.; Sykes, B. D.; Richards, F. M. *J. Mol. Biol.* **1991**, *222*, 311.
83. Catalano, M.; Ragona, L.; Molinari, H.; Tava, A.; Zetta, L. *Biochemistry* **2003**, *42*, 2836.
84. Baxter, N. J.; Williamson, M. P. *J. Biomol. NMR* **1997**, *9*, 359.
85. Cierpicki, T.; Otlewski, J. *J. Biomol. NMR* **2001**, *21*, 249.
86. Cierpicki, T.; Zhukov, I.; Byrd, R. A.; Otlewski, J. *J. Magn. Reson.* **2002**, *157*, 178.
87. Domingo, G. J.; Leatherbarrow, R. J.; Freeman, N.; Patel, S.; Weir, M. *Int. J. Pept. Protein Res.* **1995**, *46*, 79.
88. Miles, S. M.; Leatherbarrow, R. J.; Marsden, S. P.; Coates, W. J. *Org. Biomol. Chem.* **2004**, *2*, 281.
89. Jaulent, A. M.; Brauer, A. B.; Matthews, S. J.; Leatherbarrow, R. J. *J. Biomol. NMR* **2005**, *33*, 57.
90. McBride, J. D.; Freeman, N.; Domingo, G. J.; Leatherbarrow, R. J. *J. Mol. Biol.* **1996**, *259*, 819.
91. Watson, E. M. Ph.D. Thesis, University of London, 2003.
92. Marx, U. C.; Korsinczky, M. L. J.; Schirra, H. J.; Jones, A.; Condie, B.; Otvos, L., Jr.; Craik, D. J. *J. Biol. Chem.* **2003**, *278*, 21782.
93. Korsinczky, M. L.; Schirra, H. J.; Rosengren, K. J.; West, J.; Condie, B. A.; Otvos, L.; Anderson, M. A.; Craik, D. J. *J. Mol. Biol.* **2001**, *311*, 579.
94. Schwarzinger, S.; Kroon, G. J.; Foss, T. R.; Wright, P. E.; Dyson, H. J. *J. Biomol. NMR* **2000**, *18*, 43.
95. Schmidt, A.; Jelsch, C.; Ostergaard, P.; Rypniewski, W.; Lamzin, V. S. *J. Biol. Chem.* **2003**, *278*, 43357.